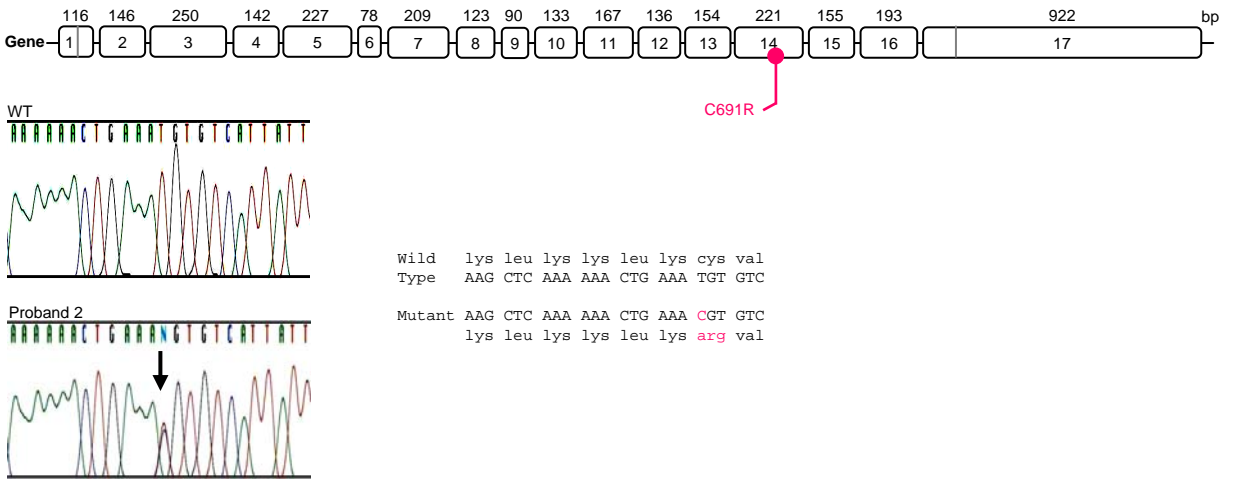
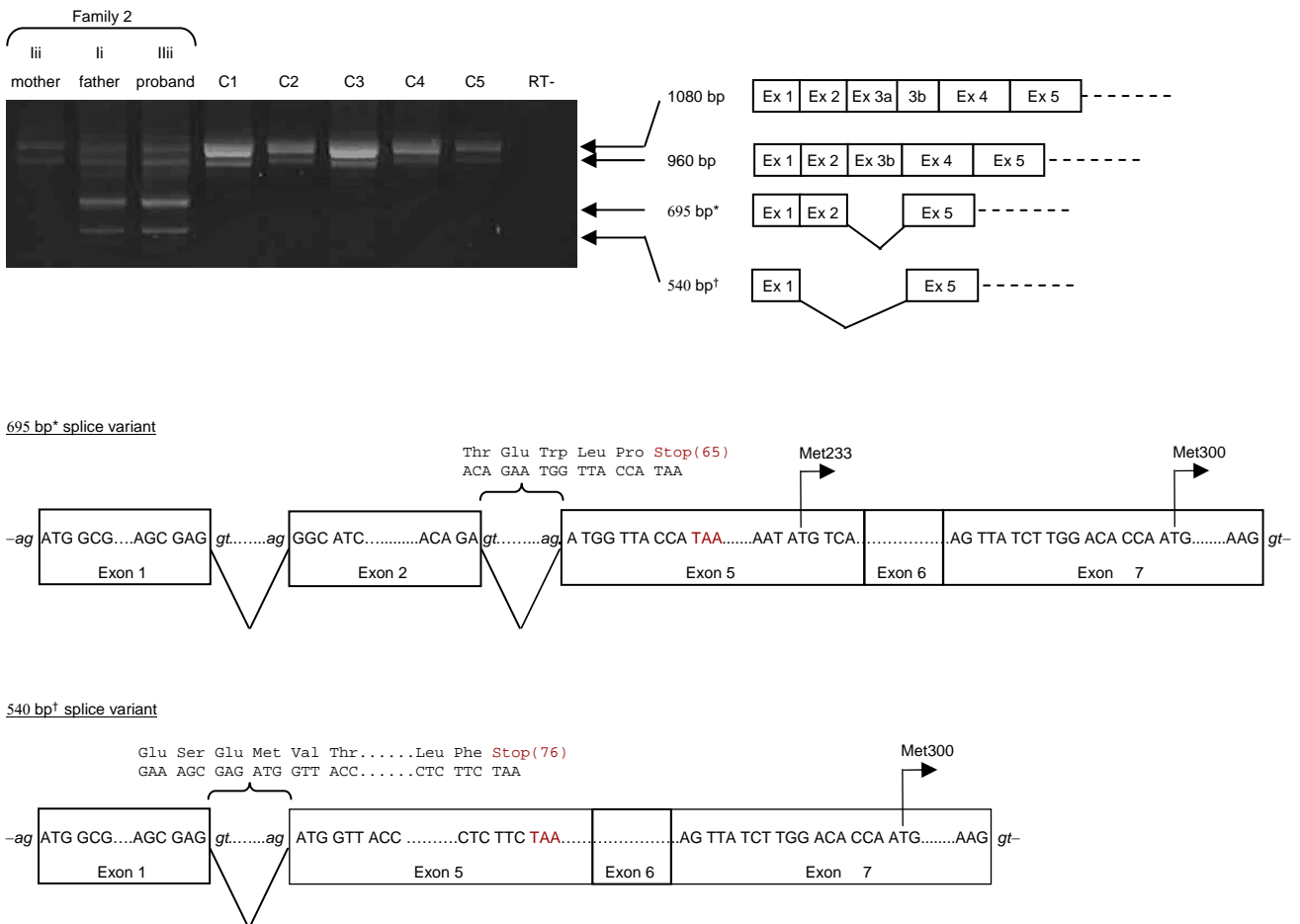


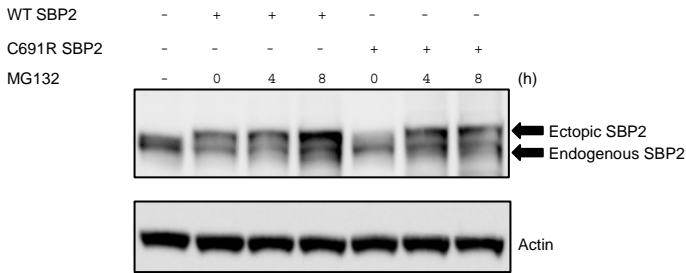
D



E

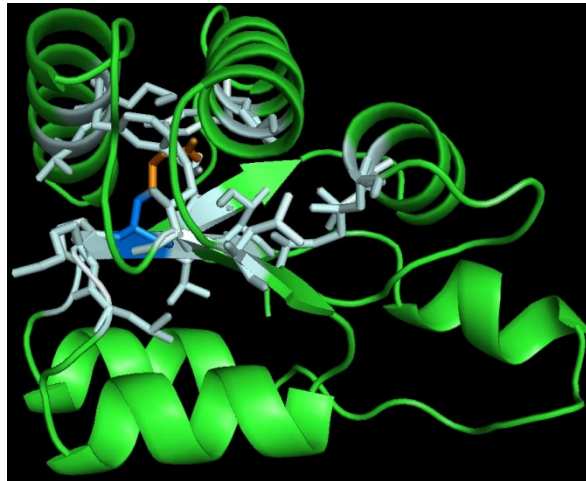


**F**

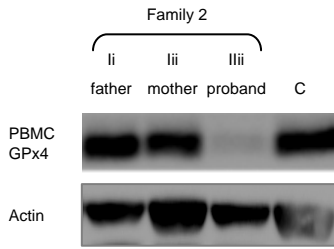


**G**

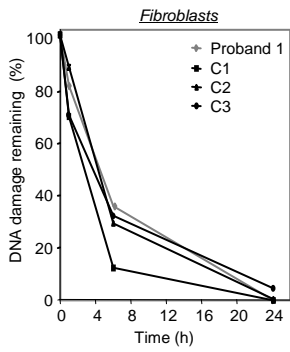
Human	SBP2 648	LLKELVRFQDRM	V	Q	K	D	P	V	K	A	K	T	K	R	R	I	V	L	G	L	R	E	V	L	K	H	L	K	L	K	L	K	C	V	I	I	S	P	N	C	E	K	I	Q	S	K	G	L	D	D	T	L	H	T	I	I	D	Y	A	C	E	Q	N	I	P	F	V	F	A	L	N	R	K	A	L	G	R	S	L	N	K	A	V	P	V	S	V	G	I	F	S	Y	D	G	A	Q	D	F	H	K	M	V	E	L	T	V	A	A	R
Macaca mulatta	SBP2 650	LLKELVRFQDRM	V	Q	K	D	P	V	K	A	K	T	K	R	R	I	V	L	G	L	R	E	V	L	K	H	L	K	L	K	L	K	C	V	I	I	S	P	N	C	E	K	I	Q	S	K	G	L	D	D	T	L	H	T	I	I	D	Y	A	C	E	Q	N	I	P	F	V	F	A	L	N	R	K	A	L	G	R	S	L	N	K	A	V	P	V	S	V	G	I	F	S	Y	D	G	A	Q	D	F	H	K	M	V	E	L	T	V	A	A	R
Pan troglodytes	SBP2 777	LLKELVRFQDRM	V	Q	K	D	P	V	K	A	K	T	K	R	R	I	V	L	G	L	R	E	V	L	K	H	L	K	L	K	L	K	C	V	I	I	S	P	N	C	E	K	I	Q	S	K	G	L	D	D	T	L	H	T	I	I	D	Y	A	C	E	Q	N	I	P	F	V	F	A	L	N	R	K	A	L	G	R	S	L	N	K	A	V	P	V	S	V	G	I	F	S	Y	D	G	A	Q	D	F	H	K	M	V	E	L	T	V	A	A	R
Canis lupus familiaris	SBP2 643	LLKELVRFQDRM	V	Q	K	D	P	V	K	A	K	T	K	R	R	I	V	L	G	L	R	E	V	L	K	H	L	K	L	K	L	K	C	V	I	I	S	P	N	C	E	K	I	Q	S	K	G	L	D	D	T	L	H	T	I	I	D	Y	A	C	E	Q	N	I	P	F	V	F	A	L	N	R	K	A	L	G	R	S	L	N	K	A	V	P	V	S	V	G	I	F	S	Y	D	G	A	Q	D	F	H	K	M	V	E	L	T	V	A	A	R
Bos taurus similar to	SBP2 645	LLKELVRFQDRM	V	Q	K	D	P	V	K	A	K	A	K	R	R	I	V	L	G	L	R	E	V	L	K	H	L	K	L	K	L	K	C	V	I	I	S	P	N	C	E	K	I	Q	S	K	G	L	D	D	T	L	H	T	I	I	D	Y	A	C	E	Q	N	I	P	F	V	F	A	L	N	R	K	A	L	G	R	S	L	N	K	A	V	P	V	S	V	G	I	F	S	Y	D	G	A	Q	D	F	H	K	M	V	E	L	T	V	A	A	R
Mus musculus	SBP2 653	LLKELVRFQDRM	V	Q	K	D	P	V	K	A	K	T	K	R	R	I	V	L	G	L	R	E	V	L	K	H	L	K	L	K	L	K	C	V	I	I	S	P	N	C	E	K	I	Q	S	K	G	L	D	D	T	L	H	T	I	I	D	C	A	C	E	Q	N	I	P	F	V	F	A	L	N	R	K	A	L	G	R	S	L	N	K	A	V	P	V	S	V	G	I	F	S	Y	D	G	A	Q	D	F	H	K	M	V	E	L	T	V	A	A	R
Rattus norvegicus	SBP2 641	LLKELVRFQDRM	V	Q	K	D	P	V	K	A	K	T	K	R	R	I	V	L	G	L	R	E	V	L	K	H	L	K	L	K	L	K	C	V	I	I	S	P	N	C	E	K	I	Q	S	K	G	L	D	D	T	L	H	T	I	I	D	C	A	C	E	Q	N	I	P	F	V	F	A	L	N	R	K	A	L	G	R	S	L	N	K	A	V	P	V	S	V	G	I	F	S	Y	D	G	A	Q	D	F	H	K	M	V	E	L	T	V	A	A	R
Sus scrofa similar to	SBP2 643	LLKELVRFQDRM	V	Q	K	D	P	V	K	A	K	T	K	R	R	I	V	L	G	L	R	E	V	L	K	H	L	K	L	K	L	K	C	V	I	I	S	P	N	C	E	K	I	Q	S	K	G	L	D	D	T	L	H	T	I	I	D	Y	A	C	E	Q	N	I	P	F	V	F	A	L	N	R	K	A	L	G	R	S	L	N	K	A	V	P	V	S	V	G	I	F	S	Y	D	G	A	Q	D	F	H	K	M	V	E	L	T	V	A	A	R
Equus caballus similar	SBP2 758	LLKELVRFQDRM	V	Q	K	D	P	V	K	A	K	T	K	R	R	I	V	L	G	L	R	E	V	L	K	H	L	K	L	K	L	K	C	V	I	I	S	P	N	C	E	K	I	Q	S	K	G	L	D	D	T	L	H	T	I	I	D	Y	A	C	E	Q	N	I	P	F	V	F	A	L	N	R	K	A	L	G	R	S	L	N	K	A	V	P	V	S	V	G	I	F	S	Y	D	G	A	Q	D	F	H	K	M	V	E	L	T	V	A	A	R
Gallus gallus	SBP2 695	LLKELVRFQDRM	V	Q	K	D	P	V	K	A	K	T	K	R	R	I	V	M	G	L	R	E	V	L	K	H	L	K	L	K	L	K	C	V	I	I	S	P	N	C	E	K	I	Q	S	K	G	L	D	E	T	L	H	N	I	D	C	A	C	E	Q	N	I	P	F	V	F	A	L	N	R	K	A	L	G	R	C	V	N	K	A	V	P	V	S	V	G	I	F	S	Y	D	G	A	Q	D	F	H	R	M	V	Q	L	T	T	E	A	R	
Taeniopygia guttata predicted	716	LLQELVSPQERI	V	Y	Q	K	D	P	T	R	A	K	A	R	R	I	V	M	G	L	R	E	V	T	K	H	M	L	N	K	C	V	I	I	S	P	N	C	E	K	I	Q	S	K	G	L	D	E	A	L	Y	N	V	I	A	M	A	R	E	Q	E	I	P	F	V	F	A	L	G	R	K	A	L	G	R	C	V	N	K	L	V	P	V	S	V	G	I	F	N	Y	S	G	A	E	D	L	K	L	V	S	L	T	E	A	R				
X. Tropicalis hypothetical	355	LLKELVRFQDRM	V	L	F	L	K	E	P	A	K	A	K	S	K	R	I	V	M	G	L	R	E	V	L	K	L	K	L	K	C	V	I	I	S	P	N	C	E	K	I	Q	S	K	G	L	D	D	T	L	H	T	I	I	S	H	A	C	E	Q	N	I	P	F	V	F	A	L	N	R	K	A	L	G	R	C	L	N	K	A	V	P	V	S	V	G	I	F	S	Y	D	G	A	Q	D	F	H	K	L	C	E	L	T	V	Q	A	R		
B. floridae hypothetical	221	LLQDLVRFQDRM	V	H	K	D	P	I	K	A	K	A	K	R	R	I	V	M	G	L	R	E	V	T	K	H	L	K	L	K	L	C	V	I	I	A	P	N	L	E	K	I	Q	S	K	G	L	D	D	A	I	E	T	I	L	N	L	C	M	E	Q	D	V	F	V	F	A	L	G	R	K	A	L	G	R	A	V	N	K	L	V	P	V	S	V	G	I	F	N	Y	D	G	A	E	E	H	F	T	M	V	E	L	T	T	Q	A	R		
M domestica similar	SBP2 764	LLKELVRFQDRM	V	Q	K	D	P	V	K	A	K	T	K	R	R	I	V	M	G	L	R	E	V	L	K	H	L	K	L	K	L	K	C	V	I	I	S	P	N	C	E	K	S	K	S	K	G	L	D	E	T	L	H	T	I	I	D	Y	A	C	E	Q	N	I	P	F	V	F	A	L	N	R	K	A	L	G	R	S	V	N	K	V	P	V	S	V	G	I	F	S	Y	D	G	A	Q	D	F	H	K	M	L	T	A	R					



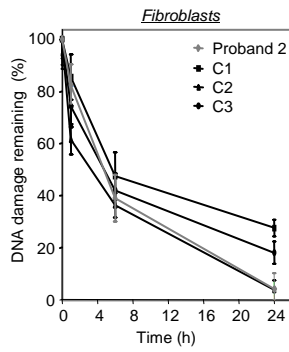
**A**



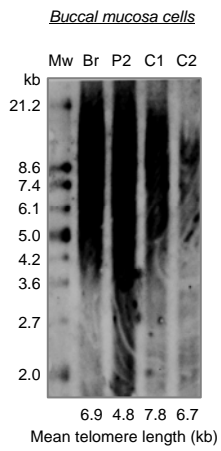
**B**



**C**

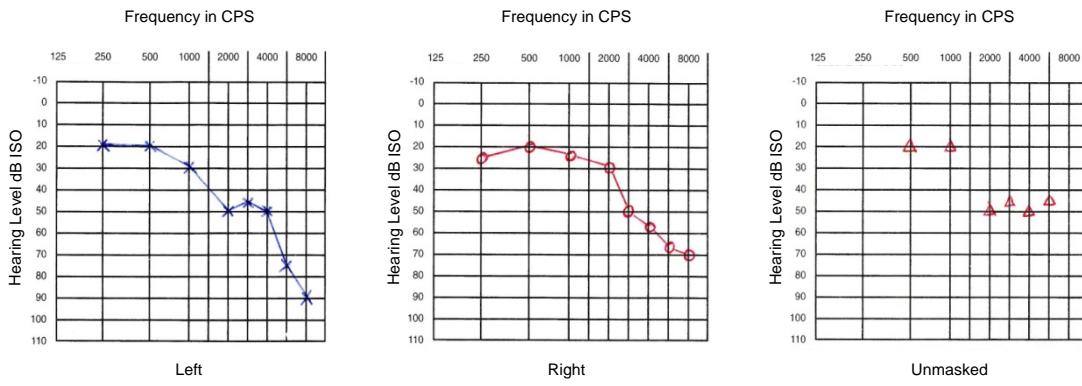


**D**



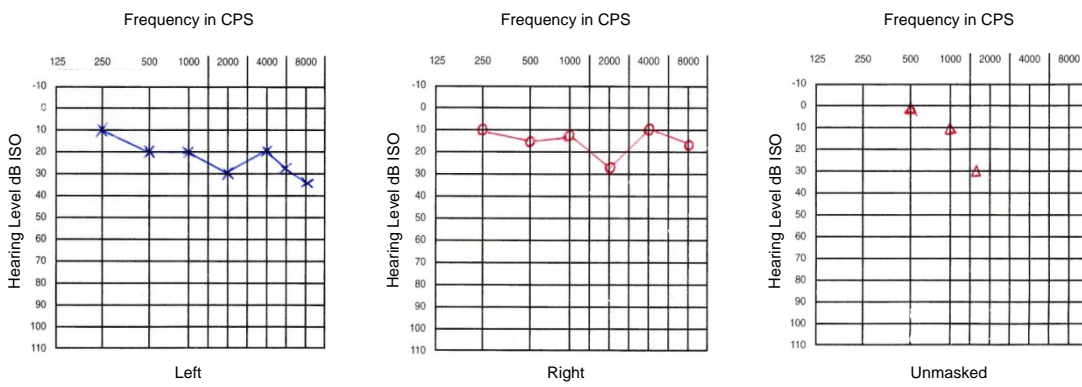
**A**

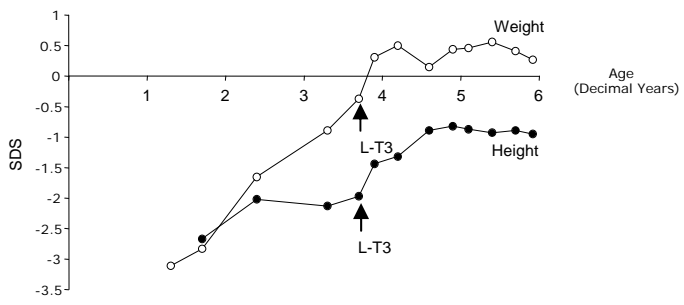
Proband 1



**B**

Proband 2





## Supplemental Data – Figure Legends

### **Supplementary Figure 1.**

**A)** Identification of a frameshift/ premature stop *SECISBP2* mutation in Proband 1. A schematic representation (top) shows organisation of the *SECISBP2* gene with exons, start and stop codons indicated. Electropherograms (left) of wild type (upper) and Proband 1 (lower) sequences, showing a heterozygous single nucleotide deletion [T668ΔT]. Alignment of wild type and mutant SBP2 protein sequences (right) indicate that this mutation shifts the reading frame at codon 223, altering subsequent residues (blue) and generating a premature stop codon at position 255.

**B)** Aberrantly spliced SBP2 transcripts in Proband 1. RT-PCR of PBMC mRNA isolated from a Control (C), the Father (Ii), the Mother (Iii) and Proband 1 (Iiii) (RT-: negative control) using a forward (exon 4) and reverse (intron 6) primers generates products only in P1. Sequencing of the two bands in P1 of 662bp (\*) and 531bp (†), indicated that they represent aberrantly spliced SBP2 transcripts. Translation of aberrantly spliced sequences (\* and †), predicts premature termination of translation at stop codons within subsequent pseudoexons (dotted boxes). The location of a single nucleotide change (t to a at -155bp) which occurs “de novo” in Proband 1 and could be linked to the splicing defect is highlighted in red. An alternative ATG codon in exon 7 (Met 300), which could direct reinitiation of protein synthesis is indicated.

**C)** Western blotting of untransfected (MOCK) or wild type (WT) or mutant (T668ΔT) *SECISBP2* minigene construct-expressing HEK293 cells. Bands corresponding to full length (FLSBP2) and shorter (ATG233, ATG300) isoforms of SBP2, generated from the downstream start codons in exons 5 and 7, are indicated (arrows).

**D)** Identification and cellular expression of a missense *SECISBP2* mutation in Family 2. Upper panel: Schematic representation of the organisation of *SECISBP2* as in (A). Wild type and Proband 2 sequences (right) indicate a heterozygous single nucleotide mutation (TGT to CGT) corresponding to a Cys to Arg change at codon 691 (left).

**E)** Aberrantly spliced SBP2 transcripts in Family 2. RT-PCR of PBMC RNA from the mother (Iii), father (Ii), Proband 2 (IIii) and five controls (C1-5), using forward (exon 1) and reverse (exon 7) primers generates different products. Two ubiquitous bands (1080bp and 960bp correspond to known, natural splice variants of SBP2; additional bands (695bp (\*) and 540bp (†), were aberrantly spliced variants only found in Proband 2 and his father. Translation of aberrantly spliced variant (\* and †) sequences, predicts premature termination of translation at stop codons (65, 76) in exon 5 (red). ATG codons in exon 5 (Met 233) or exon 7 (Met 300) downstream of this, which could be sites for reinitiation of protein synthesis are indicated. Recognised SNPs (rs3763616, rs3763617, rs67702746, rs79920679, rs11304620) were identified in Proband 2.

**F)** Western blot of 293 cells transfected with either empty, wild type (WT SBP2) or mutant SBP2 (C691R SBP2) with or without varying (0 to 8h) exposure to a proteasome inhibitor (MG132). Bands corresponding to endogenous and ectopically expressed SBP2 are indicated, with actin expression as a loading control.

**G)** Structural modelling of the C691R SBP2 mutant. Top: alignment of SBP2 sequences from different species showing conservation of Cys 691 (red) and neighbouring residues (cyan) forming a hydrophobic core. Below: modelling of the RNA binding domain of SBP2 generated by homology with the structure of L7Ae sRNP (1) using the Phyre server (2). Side chains of hydrophobic core residues (cyan)



and the amino acids at codon 691 in either wild type (Cys, dark blue) or mutant (Arg, orange) SBP2 proteins are indicated.

**Supplementary Figure 2.**

**A)** Western blotting of PBMCs from Proband 2, his father, mother and a healthy age- and gender-matched control (C) for GPx4 expression with actin as loading control.

**B and C)** Dermal fibroblasts of Probands 1 and 2 exhibit normal rates of DNA repair. Residual DNA damage following H<sub>2</sub>O<sub>2</sub> exposure (50μM, 30mins), determined at 0, 6 and 24 hours by hOGG1-modified COMET assay (see methods) in fibroblasts from proband 1 (**B**) and 2 (**C**), and age- and sex-matched control subjects (C1-3). Results, expressed as percentage damage remaining, represent the mean ± s.e.m. of 3 independent experiments.

**D)** Average telomere fragment length (kb) determined by southern blotting of DNA from buccal mucosal cells from Proband 2 (P2), his unaffected brother (Br) and two age- and gender-matched control subjects (C1, C2) using a telomere-specific probe. Mw, molecular weight size marker.

**Supplementary Figure 3.** Bilateral hearing loss in both Probands. Audiograms showing thresholds (dB) at which auditory stimuli of varying frequency (CPS) were heard in left and right ears are shown in either Proband 1 (**A**) or Proband 2 (**B**). The far right panels (unmasked) show reduced bone conduction, confirming a sensorineural basis for the hearing loss.

**Supplementary Figure 4.** Growth of Proband 2 before and after L-T3 therapy. Height (solid circles) and weight (open circles) standard deviation scores (SDS) are

plotted against age (yrs), denoting (arrowed) the point at which L-T3 treatment was started.

#### Supplementary References

1. Charron C, Manival X, Charpentier B et al. Purification, crystallisation and preliminary X-ray diffraction data of L7Ae sRNP core protein from *Pyrococcus abyssi*. *Acta Crystallogr D Biol Crystallogr*. 2004;60: 122-4.
2. Kelley LA and Sternberg MJ. Protein structure prediction on the Web: a case study using the Phyre server. *Nat Protoc*. 2009;4:363-371.

**Supplementary Table 1** Details of primers used for amplification and sequencing of the coding region of human *SECISBP2* (1-17) and 1350bp upstream of exon 1 including the core promoter region (P1-P5).

EXON	Forward primer (5'- 3')	Reverse primer (5'- 3')
1	CGTACTTCCGGCCGGAAGAA	TGCCGTCACCAGCATCCGA
2	TGGGGCTATTAGGAACACCTC	CCAAAATGTAAGCCCCTAGGTA
3	CTGGAGCATCTTCTGGCTCT	AAAGCAACCAACTAAAGGACACA
4	TTTTGCTGCTTTAAACCTTTTT	TTCTGGGGCACAAGGAGTAG
5	TCTGCAATTTTTGCTTGCAT	CAAAGCCCACAGCAAGATTT
6	TTCTGTTGTCAAAGTGTCTGGA	CAACAAAAATCATTTCAACTGC
7	GCTCTGAGCAGTTACCTCATGT	CTGGCAACCACCATCCTACT
8	ACCGCCCTAAAAACAGGATT	GGAAACCAATATGAACCCAAG
9	AGGTTGCACTTGGATGTTT	TCAAGCATTTAGTTGAGCCAGA
10	TTTGTA AAAAGAAAAGCACAGTTTG	AACTTTTGATAACAAGAGAAAATGG
11	GAGCTGCGATCCAAGAGC	GAGCTGGGAGAATAACTATGGAAA
12	ACAAGTATTTAGGCATTTTAATTGTTT	GTCAGCCAAGTCCTGGAGAG
13	ATCGGTGAGACTGCATTGG	ATGCCATACTGAACCGAAGC
14	CTGCAGTGTACAGCCAGT	AAACACGAGGGCACACTAGG
15	GGGTGTGTTGCTAAGAAAAAGC	GTGAGCCCACACTGACCAC
16	ACCCGTGTCTCTGTAGCTG	AGCATTGTCAAGCTGCTCAC
17	CCTCTCTCATGCTGCTGGTT	TCATGTGCCCTTTAATGCTG
P1	TGCTATAGAAACATCTTAAATGAGCAG	GTCCTGGTGGGTCTCAGTTC
P2	AAAGGAAGGCGACAGCTACC	CAGGGATAGGAGGTTGACCA
P3	CAAGCCTTTGAGTGAGAGGAA	CTCTCGCTGAGGTGACCTTT
P4	AATCTCGGCCTCCTCAGTTT	CTTGCCGGACAGACAAAGC
P5	GTCCCCATTTTCCGCAAG	GGCCCTTACCTCGCTTTC

**Supplementary Table 2** Details of qPCR probes and observed fold differences in gene expression for a panel of selenoproteins of unknown function in dermal fibroblasts of probands 1 and 2 compared with unaffected control fibroblasts (data corresponds to heat maps shown in Figure 11).

Gene	Probe	Fold difference	
		Proband 1	Proband 2
<i>SELH</i>	Hs00415057_m1	-7.00	-3.42
<i>SELW</i>	Hs01071062_m1	-2.16	-1.69
<i>SELT</i>	Hs00892526_g1	-1.33	-1.20
<i>SELM</i>	Hs01115694_g1	1.37	1.15
<i>SELO</i>	Hs00972565_g1	1.30	2.39
<i>SELI</i>	Hs01013816_m1	1.71	1.83
<i>SELK</i>	Hs00431229_g1	1.06	2.45